Oyster Flood Tracker Project: Reconstructing Inflows to Reefs and Effects on *Vibrio vulnificus* and *Perkinsus marinus* Abundance

Publication CBBEP – 136
Project Number – 1920
August 2019

Prepared by

Benjamin Walther, Principal Investigator
Jeffrey Turner, Co-Principal Investigator
Paxton Bachand, Field Supervisor & Lab/Data Manager
Colin O'Donnell, Lab Technician
Andrew Hinson, Lab Technician
Texas A&M University – Corpus Christi
6300 Ocean Drive, Unit 5800
Corpus Christi, Texas 78412

Submitted to:
Coastal Bend Bays & Estuaries Program
615 N. Upper Broadway, Suite 1200
Corpus Christi, TX 78401

The views expressed herein are those of the authors and do not necessarily reflect the views of CBBEP or other organizations that may have provided funding for this project.

Oyster Flood Tracker Project: Reconstructing Inflows to Reefs and Effects on *Vibrio vulnificus* and *Perkinsus marinus* abundance

FINAL REPORT

Prepared by:
Benjamin Walther, Principal Investigator
Jeffrey Turner, Co-Principal Investigator
Paxton Bachand, Field Supervisor & Lab/Data Manager
Colin O'Donnell, Lab Technician
Andrew Hinson, Lab Technician
Texas A&M University – Corpus Christi
6300 Ocean Drive, Unit 5800
Corpus Christi, Texas 78412
Phone: (361) 825-4168
E-mail: benjamin.walther@tamucc.edu

CBBEP Project Manager: Rosario Martinez

SUBMITTED TO:

Coastal Bend Bays & Estuaries Program
615 N. Upper Broadway, Suite 1200
Corpus Christi, TX 78401

The views expressed herein are those of the authors and do not necessarily reflect the views of CBBEP or other organizations that may have provided funding for this project.

TABLE OF CONTENTS

ABBREVIATIONS

ATCC	American Type Culture Collection
CBBEP	Coastal Bend Bays & Estuaries Program
CFU	Colony Forming Unit
DF	Dilution Factor
DO	Dissolved Oxygen
IAEA	International Atomic Energy Agency
IRMS	Isotope Ratio Mass Spectrometry
NERR	National Estuarine Research Reserve
NIST	National Institutes of Standards and Technology
PBS	Phosphate Buffered Solution
PCR	Polymerase Chain Reaction
QAPP	Quality Assurance Project Plan
SCB	St. Charles Bay
SHR	Shellbank Reef
TAMU-CC	Texas A&M University at Corpus Christi
TCEQ	Texas Commission on Environmental Quality
TSB	Tryptic Soy Broth
UCD-SIF	University of California Davis Stable Isotope Facility
VPDB	Vienna PeeDee Belemnite
vvhA	*Vibrio vulnificus* hemolysin A
VVX	*Vibrio vulnificus* X-Gal

SUMMARY

Punctuated flood events, such as those during Hurricane Harvey, bring large amounts of fresh water to oyster reefs which can have profound implications for oyster physiological stress and loading of harmful bacteria and parasites. Previous studies have shown that drought-induced salinity fluctuations affect the abundance of *Vibrio vulnificus* and *Perkinsus marinus* in oysters. However, the effects of salinity fluctuations associated with periodic freshwater pulses are unknown. To assess the effects of freshwater pulses, this study accomplished two goals: 1) reconstructed a reef-specific history of freshwater pulses (i.e., salinity fluctuations) through stable isotope analysis, 2) quantified the abundance of *V. vulnificus* and *P. marinus* through culture-dependent and culture-independent microbiology analyses. The degree to which freshwater pulses alter oyster vulnerability to harmful bacteria and parasites is currently underappreciated yet important to effectively inform oyster restoration and conservation.

This work compared infection dynamics and isotope histories in oysters from two locations, Shellbank Reef and St. Charles Bay. These sites were initially chosen for their potential differences in environmental conditions, however salinity and temperature histories in the year prior to the project were similar in magnitudes of fluctuations and timing of salinity changes due to regional climate conditions, although minimal and maximal salinities were marginally different among sites. As a result, isotope histories were also comparable between sites with no major differences identified in temporal patterns or averages among shells from both sites. However, this result indicated that both the natural (St. Charles Bay) and restored (Shellbank Reef) sites experienced similar fluctuations in environmental conditions. *V. vulnificus* and *P. marinus* were detected throughout the study but the abundance of these microorganisms was not correlated with environmental parameters or one another. Importantly, the *P. marinus* infection intensity was always lower in Shellbank Reef, which suggests that restored reefs experience lower infection frequencies. Together, findings indicate that restored reefs may be less vulnerable to diseases like Dermo.

ACKNOWLEDGEMENTS

We thank the Texas Commission on Environmental Quality (TCEQ) and the Coastal Bend Bays and Estuaries Program (CBBEP) for funding this study. We thank the Texas A&M University-Corpus Christi (TAMU-CC) Center for Coastal Studies for their assistance with field sampling. In particular, we thank Robert Duke and Jay Tarkington for assistance in the field. Shell stable isotope analyses were conducted at the University of California Davis Stable Isotope Facility (UCD-SIF) by Richard Doucette, and we give sincere thanks for his expertise and guidance on this portion of the project. We also thank Dr. Jennifer Beseres Pollack and her Research Associate Natasha Breaux (TAMU-CC Harte Research Institute) for conducting the Dermo analysis. This project would not have been possible without the assistance and expertise of graduate and undergraduate students at TAMU-CC: Paxton Bachand, Colin O'Donnell, and Andrew Hinson.

INTRODUCTION

The purpose of the proposed project was to assess how variation in freshwater inflow affects the abundance of *Vibrio vulnificus* and *Perkinsus marinus* in oysters from St. Charles and Copano Bays. Punctuated flood events, such as those during Hurricane Harvey, bring large amounts of freshwater to oyster reefs which can have profound implications for oyster physiological stress and loading of harmful bacteria and parasites. A previous study has shown that a drought-induced increase in salinity eliminated *V. vulnificus* in oysters (Froelich *et al.* 2012), and a separate study has shown that *P. marinus* abundance is strongly linked to higher salinities (Pollack *et al.* 2012). However, the effects of salinity fluctuations associated with periodic freshwater pulses (e.g., storm runoff) are unknown. Assessing links between inflows and *V. vulnificus* and *P. marinus* requires time series of salinity variations at the reef scale, which are often unavailable from instrumental monitoring. Fortunately, oyster shells themselves naturally record salinity fluctuations via stable isotope ratios of oxygen and carbon that are incorporated into shell growth increments. Thus, each oyster shell contains a record of the frequency, duration, and magnitude of salinity variability in response to flood events over the course of the oyster's life. Pairing this individual record of salinity stress with assessments of *V. vulnificus* and *P. marinus* abundance is a powerful step forward in identifying the effects of inflow patterns on important estuarine resources.

Stable isotope ratios ($\delta^{18}O$ and $\delta^{13}C$) in estuarine bivalve shells can be effective proxies for salinity and temperature over time (Gillikin *et al.* 2006; Surge *et al.* 2001). The use of $\delta^{18}O$ and $\delta^{13}C$ together help resolve the combined effects of temperature and salinity and therefore distinguish droughts and floods, where significant flood events cause simultaneous drops in $\delta^{18}O$ and $\delta^{13}C$ values with the delivery of freshwater and terrestrial carbon. This phenomenon was recently validated for oyster shells in Mission-Aransas Bay (Walther and Rowley 2013). The value of these isotope time series is that the periodicity and magnitude of salinity depression associated with flood events can be estimated on a reef scale. This is crucial to identify stress exposure histories of individual reefs, particularly where water quality is not monitored or where monitoring stations have been lost due from winds and storm surges. Salinity histories can then be coupled with assessments of flood consequences, such as harmful bacteria and parasite abundance.

V. vulnificus is a naturally occurring marine bacterium and one of the deadliest human pathogens (Strom and Paranjpye 2000). Infections commonly follow the ingestion of oysters harboring the bacterium or the exposure of a wound to contaminated water. The abundance of the bacterium is correlated with warmer water temperatures, but the role of salinity is less obvious, although a previous study found that extreme drought-induced salinities were responsible for the loss of *V. vulnificus* in oysters (Froelich *et al.* 2012). In the warm waters of the northern Gulf of Mexico, infections have severe consequences on the seafood industry and coastal economies. A colleague at the University of Southern Mississippi (Dr. Jay Grimes) recently formulated a novel agar (*V. vulnificus* X-Gal or VVX) for the direct one-step isolation and enumeration of *V. vulnificus* from oyster tissue (Griffitt and Grimes 2013). In addition to harmful bacteria, oysters are subject to infection by the Dermo-causing parasite *P. marinus*. Dermo disease can cause significant mortality and loss of oysters, and disease progression is severe at higher salinities (Pollack *et al.* 2012). Linking salinity histories with *V. vulnificus* and *P. marinus* abundance can provide novel insight into flood-driven oyster pathology dynamics.

Data identifying the impacts of freshwater inflows on oysters are imperative to effectively manage this species that provides valuable ecosystem services as well as fishery resources to local

communities. The degree to which floods alter oyster vulnerability to harmful bacteria and parasites is currently underappreciated yet important for oyster conservation and restoration and human health risk assessments. Although links between salinity and *P. marinus* infection rates have been investigated, the impacts of salinity histories (i.e., the reconstruction of salinity fluctuations of an oyster's life history) have yet to be evaluated. This project brought together a novel combination of approaches and expertise: bacterial pathogen analysis to identify *V. vulnificus* presence (Turner *et al.* 2014), assessment of *P. marinus* infection intensities, and isotope analyses to construct shell-specific salinity fluctuation histories (Walther and Rowley 2013). The combination of these techniques provided a unique insight into the impacts of flooding on harmful bacteria and parasites.

This study had two primary goals: 1) reconstruct a reef-specific history of freshwater pulses (i.e., salinity fluctuations) through stable isotope analysis, 2) quantify the abundance of *V. vulnificus* and *P. marinus* through culture-dependent and culture-independent microbiology analyses. This work was carried out in two locations with different reef types: St. Charles Bay (where we sampled natural reefs) and Shellbank Reef in Copano Bay (where we sampled restored reefs). We were thus able to compare salinity histories and pathogen infection patterns between natural and restored reefs in close proximity to one another to assess if pathogen susceptibility differs among these reef types. This project thus has relevance for ongoing reef restoration strategies in Texas.

METHODS

Environmental Parameters

Oysters collections occurred during five sampling events (04/08/2019, 04/29/2019, 05/29/2019, 07/09/2019, and 07/29/2019). At each collection event, a YSI 556 Handheld Multiparameter Instrument (YSI Incorporated, Yellow Springs, OH) was used to measure water temperature (ºC), specific conductivity (µmhos/cm), salinity (ppt), pH (s.u.), and dissolved oxygen (% saturation and mg/L). These water quality parameters were recorded at each collection event from both sites.

In order to compare long-term water quality parameters to shell time series, salinity and ambient water temperature measurements were retrieved from water quality monitoring stations maintained by the Mission Aransas National Estuarine Research Reserve (NERR) and accessed online via the NERR Centralized Data Management Office website (https://cdmo.baruch.sc.edu/). Parameter measurements were retrieved for the two year period prior to the current study from 05/29/2017 to 5/29/2019 from two stations: Copano Bay East (Station ID MARCEWQ) and Copano Bay West (Station ID MARCWWQ) to obtain records in close proximity to oyster sampling locations. At these stations, temperature and salinity measurements are recorded every 15 minutes when sensors are operational. To reduce the temporal resolution of these measurements, daily averages of salinity and water temperature were calculated. On several occasions, the water quality stations experienced technical issues causing gaps in their records. If only one 15-minute measurement was missing from a 24-hour period, the remaining measurements for that day were used to calculate the daily average. If more than one 15-minute measurement was missing, then that day was excluded from the average calculations and the day was considered 'missing'. In general, the absence of more than one 15-minute measurement indicated sensor malfunction for an extended period of time (days to weeks). The largest gap in measurements occurred at Copano Bay East, likely as a result of Hurricane Harvey, leaving a gap from 08/09/2017 to 06/23/2018.

Oyster Sampling

A total of 40 Eastern oysters (*Crassostrea virginica)* were collected from two sites, Shellbank Reef in Copano Bay (Latitude N 28°6'43", Longitude W 97°9'6") and St. Charles Bay (Latitude N 28.139476, Longitude W -96.969699) (Figure 1).

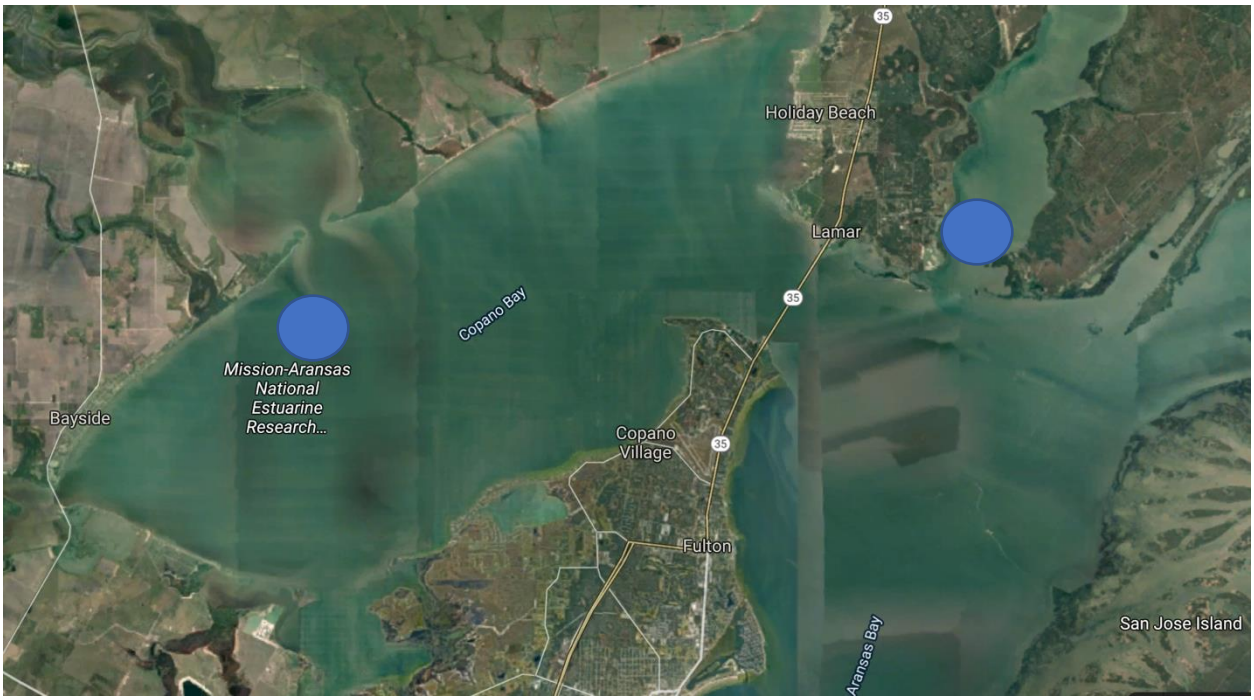

Figure 1. Map of sampling sites where oysters were collected from Shellbank Reef in Copano Bay and St. Charles Bay.

Oysters were collected by way of a dredge over the course of five sampling events (04/08/2019, 04/29/2019, 05/29/2019, 07/09/2019, and 07/29/2019). Each individual sampling event involved the collection of four oysters from Shellbank Reef and four oysters from St. Charles Bay. Oysters were selected on the basis of the market size (shell height of 3 inches) as well as showing little to no external evidence of bore-holes, created by polychaetes and other boring snails, near the hinge of the shell. At each site, the four oysters that fulfilled these requirements were placed into plastic bags and stored in a cooler maintained between 10 and 15^{o}C. A Kestrel Drop D1 (Kestrel Instruments, Boothwyn, PA, USA) was placed inside the cooler to monitor and record the proper temperature range, and the temperature was adjusted by adding or removing ice packs. No sample was held within this temperature range for longer than six hours.

Oyster processing

The collected oysters were transported to the lab for microbiological analyses. Oysters were labeled (date-site-type-number) according to the Quality Assurance Project Plan (QAPP). To remove excess sediment, oysters were rinsed and scrubbed with 1 L seawater collected from the sampling sites. The height of each oyster shell was recorded using digital calipers (Fisher Scientific, Hampton, NH, USA). The oysters were then shucked with flame sterilized oyster knives and a 5 mm^2 (dime-sized) section of the upper mantle, near the hinge, was removed with flame sterilized scissors. The mantle samples were incubated for two weeks at room temperature in fluid thioglycollate media and the infection intensity was assigned a numerical value ranging from 0 (no infection) to 5 (heavy infection) as described previously (Ray 1952). For each oyster, the remaining oyster meat was placed in a weigh boat and the mass was recorded. Phosphate buffered saline (PBS) solution was then added to each measuring boat until the mass (oyster and PBS) was double the mass of the oyster (1:1 mass ratio). The mixture (oyster and PBS) was then

homogenized in an immersion blender until there were no visible components of the oyster. After complete homogenization, three rounds of ten-fold serial dilutions (10^{-1}, 10^{-2} and 10^{-3}) were performed by initially adding 1 mL of the homogenate into 9 mL of PBS. A 100 µL aliquot of each dilution was spread onto VVX agar plates (Griffitt and Grimes 2013) in triplicate using flame sterilized cell spreaders. The inoculated plates were incubated overnight (18-24 hours) at 30ºC. Following the incubation, plates that contained 20-200 blue colonies (presumptive *V. vulnificus*) were counted and recorded. The number of colony-forming units (CFU) was calculated according to the following formula:

CFU/mL = CFU × the dilution factor (DF)

DF = oyster dilution factor (1:1) × serial dilution factor (10^{-1}, 10^{-2} or 10^{-3}) × plating dilution factor (1:10)

For each individual oyster, up to five randomly selected blue colonies were collected and cryopreserved. For this purpose, colonies were picked with an autoclave sterilized toothpick and transferred to a test tube containing 7 mL of marine broth. The tubes were incubated overnight (18-24 hours) at 30ºC with shaking (150 rpm). The remaining untouched colonies from the dilution plates that had less than five visible blue colonies were also inoculated and incubated at 30ºC. A 750 µL sample of each overnight culture was cryopreserved (-80ºC, 20% glycerol final concentration) in 2 mL cryogenic microcentrifuge tubes.

DNA extraction

The genomic DNA from each of the above isolates was extracted using the boil lysis method as described previously (Englen and Kelley 2000). Briefly, the cryopreserved isolate was resuscitated by incubating overnight (18-24 hours) in 10 mL tryptic soy broth (TSB) at 30ºC with shaking (150 rpm). 200 µL of each overnight culture was added into 0.2 mL microcentrifuge tubes and centrifuged at 10,000 rpm for 5 minutes to form a visible pellet. The pellet was resuspended in 50 µL of sterile water and placed in Bio-Rad C1000 Touch Thermal Cycler (Bio-Rad, Richmond, California). Using the Thermal Cycler, cells were heated to 100ºC for 5 minutes and cooled to 4ºC, resulting in cell lysis and release of DNA. The extracted DNA was stored at -20ºC.

V. vulnificus confirmation

From each presumptive *V. vulnificus* isolate, the identity of the isolate was tested by polymerase chain reaction (PCR) targeting the species-specific *vvhA* gene sequence (Kaysner and DePaola 2004; see Table 1 for primer sequences). Each PCR reaction contained 5 µL of nuclease-free water, 10 µL of Qiagen fast cycle master mix, 1 µL of *vvhA*-785F, 1 µL of *vvhA*-1303R, and 3 µL of sample DNA. The PCR reactions were completed with a Bio-Rad C1000 Touch Thermal Cycler (Bio-Rad, Richmond, California) according to the cycling conditions provided in Table 2. A known strain of *V. vulnificus* (American Type Culture Collection strain 27562) was used as the positive control and nuclease-free water was used as the negative control. A positive PCR test produced a 519 bp amplicon, which was visualized by gel electrophoresis of the PCR products. The gel was made by mixing 10 µL of PCR product with 2 µL of 6x loading dye which was then loaded into a 1.5% agarose gel that contained SYBRsafe DNA stain. The gel was run at a constant voltage of 10 V/cm for 20 min. The 519 bp amplicon was visualized with a UV transilluminator.

Table 1. Primer sequences specific to *Vibrio vulnificus*.

Primers	Genomic sequence
vvhA-1303R	5' -CCG CGG TAC AGG TTG GCG CA-3'
vvhA-785F	5' -CGC CAC CCA CTT TCG GGC C- 3'

Table 2. PCR thermal cycler conditions used to quantify 519 bp amplicon specific to *Vibrio vulnificus*.

Step	Temp (^{o}C)	Time (min)	Number of Cycles
Enzyme activation (denature)	94	10	1
Denaturation	94	1	25
Annealing	62	1	25
Extension	72	1	25
Final Extension	72	10	25
Signal Stabilization	8	indefinite	1

Oyster shell sectioning and isotope analyses

Six oyster shells (three from Shellbank Reef and three from St. Charles Bay), collected 5/29/2019, were processed for isotope analyses. The two remaining shells from that collection date were not used because the hinges were broken or heavily impacted by bore holes rendering them unusable. Shells were cleaned with a brush and hot water to remove any residual oyster tissues and biofouling organisms from the exterior of each shell. All shells were air dried after cleaning prior to sectioning for isotope analyses. The shells were then mounted on an IsoMet^{TM} (Buehler, Lake Bluff, IL) low-speed saw and sectioned using a diamond wafering blade. A 4-6 mm cross-section was removed from the hinges of each shell. The cross-section was cut perpendicular to the growth lines on the oyster shell in order to capture growth increments across the entire life of each individual from spawning to collection (Figure 2).

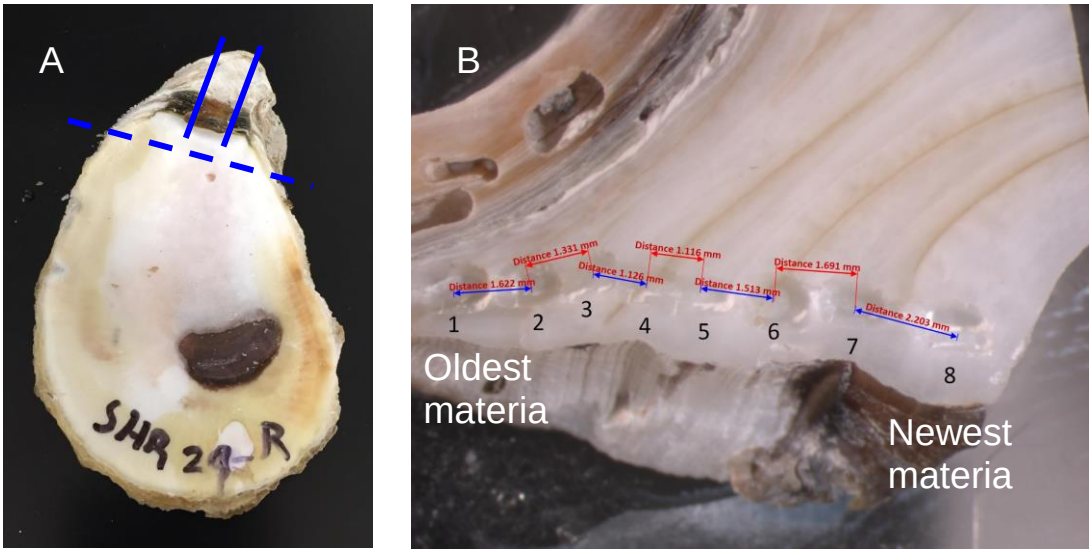

Figure 2. A) Oyster shell with lines illustrating cuts made to obtain a hinge cross-section. The first cut (dashed line) removed the hinge from the rest of the shell, while the second set of cuts (solid lines) isolated a cross-section of growth increments from the middle portion of the hinge. B) Example hinge cross-section illustrating transect of rasters across growth increments from oldest (left side of image) to newest shell material (right side).

Each cross-section was then adhered to a petrographic glass slide using cyanoacrylate glue and allowed to dry for 12-24 hours. Slides were then processed to extract sequential subsections of shell material in powdered form for isotope analyses using a New Wave Research MicroMill (Electro Scientific Industries, Inc., Portland, OR) coupled to a camera and image processing software that allowed precise designation of three-dimensional rasters for milling and removal. Milled rasters were extracted sequentially across growth increments from the foliated calcite region beneath the resilifer (the groove along the hinge where a ligament attaches and holds the two shell valves together). Sequential rasters were drilled 450 µm deep and between 1400x700 µm to 1500x900 µm wide to obtain a target mass of 1 mg of sample powder. Raster widths varied because of spatial constraints in the configuration of growth increments and the presence of holes in the shell material as a result of boring biofouling organisms on the exterior of some shells. Once milled, powder from each subsample was weighed on a Cubis MSA2.7S Ultra-Microbalance (Sartorius, Goettingen, Germany) and placed into individually labeled 1 dram glass vials for shipment to the University of California Davis Stable Isotope Facility (UCD-SIF) for analysis of $\delta^{13}C$ and $\delta^{18}O$ values. The shell surface and milling drill bit were blasted with compressed air to remove residual powder and minimize cross-contamination of shell material between subsamples. In total, 50 subsamples of powder collected across all six shells used for this project.

At UCD-SIF, subsamples of each separate milling raster were weighed to obtain approximately 0.3 mg of powder which was placed into borosilicate Labco Exetainer vials and dried to a constant weight at 100°C in an oven overnight. Dried samples were then acidified with several drops of 100% phosphoric acid to acidify the carbonate samples and liberate the CO_2 for analysis. Isotopic ratios were quantified by analysis of liberated CO_2 on a Thermo-Scientific GasBench II coupled to a Thermo-Finnigan Delta Plus XL isotope-ratio mass spectrometer (IRMS) following standardized methods (Ostermann and Curry 2000; Sharp 2007; Walther and Rowley 2013).

Duplicate samples were analyzed for 5 of the 50 samples analyzed to assess sample heterogeneity. Replicates of quality control and assurance reference materials were analyzed every 10 samples.

Certified and in-house standard reference materials were used to calibrate and report isotopic values relative to Vienna PeeDee Belemnite (VPDB) in standard δ notation (values reported in ‰). Changes in linearity and instrumental drift were accounted for with an in-house carbonate reference material (G-86). Sample values were then scale-normalized using three certified standard reference materials for carbonates (NBS 18, NBS 19 and LSVEC) obtained from the National Institute of Standards and Technology (NIST) and the International Atomic Energy Agency (IAEA). Additional certified reference materials (IAEA-603 and USGS44) and in-house reference standards (BYU-1 and UCD-SM92) were measured and used along with all reference materials to assess methodological accuracy and precision for both $\delta^{13}C$ and $\delta^{18}O$ values. Methodological precision was assessed by calculating the mean standard deviation across all measurements of the reference materials while accuracy was calculated as the mean absolute difference between measured and certified $\delta^{13}C$ and $\delta^{18}O$ values in reference materials.

The mean standard deviation for reference material replicates (an indication of instrumental precision) in this project was ±0.10‰ for $\delta^{13}C$ and ±0.10‰ for $\delta^{18}O$ values. The mean absolute accuracy for calibrated reference materials (an indication of instrumental accuracy) was ±0.05‰ for $\delta^{13}C$ and ±0.02‰ for $\delta^{18}O$ values. Both measurements indicated that instrumental precision and accuracy for the IRMS procedure were both high. The mean standard deviation for sample material replicates, however, was ±0.19‰ for $\delta^{13}C$ and ±0.49‰ for $\delta^{18}O$ values and therefore indicated poorer precision with respect to the oyster shell samples themselves. This precision loss was likely driven by sample heterogeneity within the 1 mg removed by micromilling. The possible inclusion of material across multiple growth increments (with different isotopic compositions) as well as inadvertent inclusion of non-calcitic material in subsamples milled in close proximity to a bore hole may have led to sample heterogeneity that would drive poorer precision. Regardless of the cause, variation in isotope values less than 0.2‰ for $\delta^{13}C$ and less than ±0.5‰ for $\delta^{18}O$ should be interpreted with caution given the sample precision assessments.

Isotope values for each shell were plotted against their raster distance from the oldest portion of the hinge, or umbo, to examine fluctuations in values across growth increments. Boxplots illustrating individual distributions of values for each shell were also graphed to examine internal variance across shells and between capture locations. In addition, one-way repeated measures analyses of variance were calculated separately for $\delta^{13}C$ and $\delta^{18}O$ values to determine if any statistically significant differences in either isotope value between individual shells were evident. Finally, linear regressions of $\delta^{18}O$ against $\delta^{13}C$ were fitted for each shell to investigate if variations in both isotope values were concordant across growth increments for a given shell.

RESULTS AND DISCUSSION

Environmental parameters

The environmental parameters (i.e., temperature, salinity, DO, and pH) varied minimally over the three month study (Figure 3). At Shellbank Reef, these parameters ranged from 21.98-30.31ºC, 11.15-18.28 salinity, 91.5-101.1%, and 7.9-8.16, respectively. At St. Charles Bay, these parameters ranged from 23.41-30.44ºC, 17.27-21.65 salinity, 97.0-107.5%, and 7.9-8.16, respectively. A gradual increase in temperature and salinity was observed at each site but only the

increase in temperature was correlated between the two sites ($R=0.98$, $p<0.01$). Temperature and salinity were correlated within Shellbank Reef ($R=0.93$, $p<0.05$), although a visual correlation between temperature and salinity was apparent in St. Charles Bay. The temperature and salinity ranges were optimal for the growth of both *V. vulnificus* and *P. marinus*.

Temperature and salinity patterns for the two years prior to the study indicated comparable long-term patterns between Copano West and Copano East sampling stations (Figure 4), which were close to the Shellbank Reef and St. Charles Bay sites, respectively. Average daily temperatures oscillated seasonally between summer maxima of 30-32^{o}C at both locations and winter minima of 10-11^{o}C in both locations in 2018 and 6-7^{o}C at Copano West in 2017 (the sensors were non-operational at Copano East for this time period following Hurricane Harvey damage). Average daily salinity patterns were broadly comparable between the two locations in the year prior to this study, with some differences. At Copano West, salinities peaked at 26.5 on 6/18/2018 followed by a precipitous drop to salinities of 7.7 by 6/23/2018. A slow increase in salinity followed over the subsequent months to a secondary peak of 18.6 on 9/7/2018 followed by a dramatic drop to a salinity of 1.7 by 9/20/2018. Salinities steadily increased afterwards to 14-15 by the end of May 2019. Despite the lack of data for Copano East between August 2017 through June 2018 because of Hurricane Harvey damage, subsequent temporal salinity patterns after monitoring resumed were largely similar to Copano West, although with some differences in minima and maxima. Copano East salinity peaked at 34.7 on 9/5/2018 followed by a dramatic drop to 9.3 by 9/22/2018. Salinity subsequently increased to 17-18 by May 2019. Thus, while the salinity minima and maxima were higher at Copano East by approximately 2-8 above those at Copano West, the temporal patterns in the preceding year were quite similar.

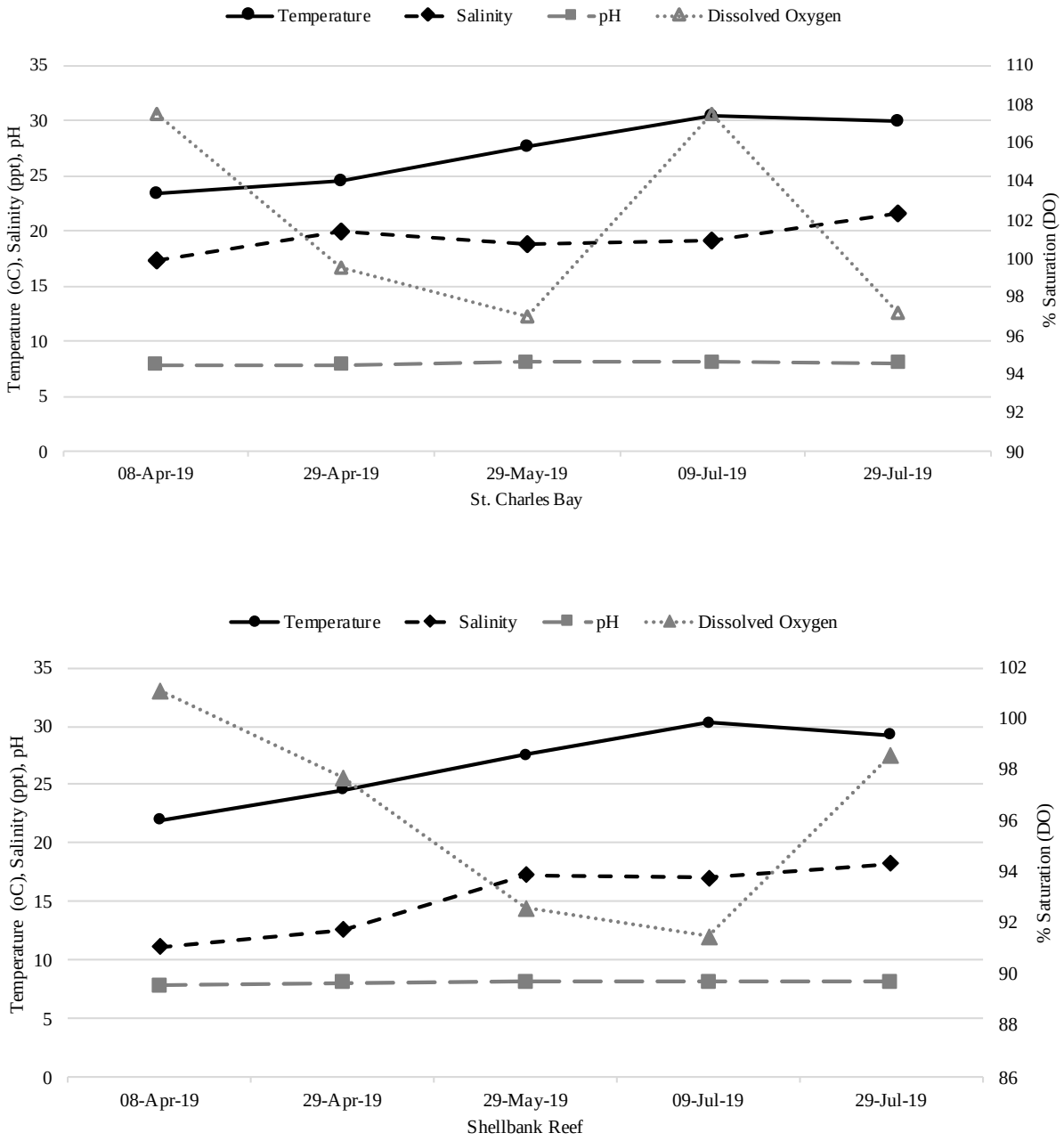

Figure 3. The variation in temperature (ºC), salinity (ppt), dissolved oxygen (% saturation), and pH recorded over the three month study period in St. Charles Bay and Shellbank Reef.

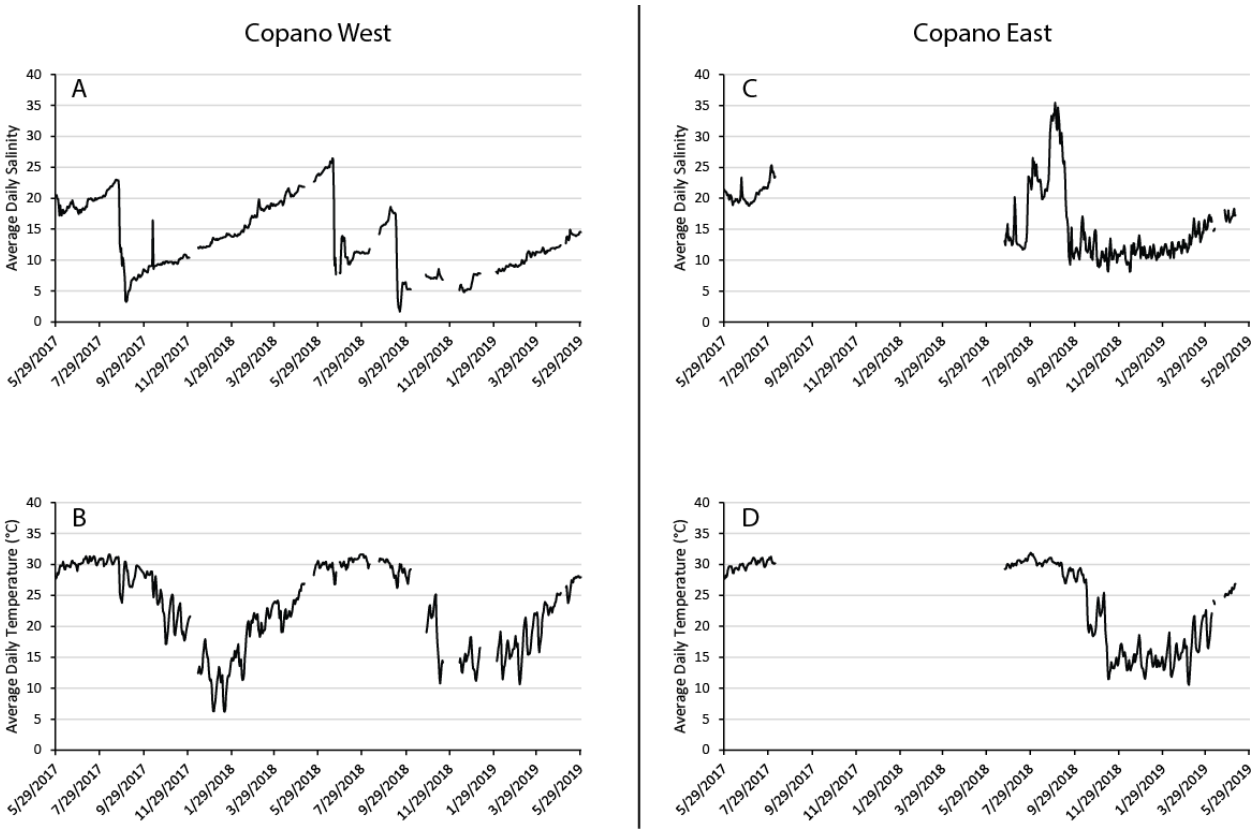

Figure 4. Time series of temperature and salinity from Mission Aransas National Estuarine Research Reserve water quality monitoring stations (A-B) Copano West and (C-D) Copano East for two years prior to this project. Gaps in the series indicate missing data due to sensor malfunctions or hurricane damage.

Oyster sampling & processing

The abundance of *V. vulnificus* varied moderately over the three month study (Figure 5). In Shellbank Reef, the abundance of presumptive *V. vulnificus* ranged from not detectable to 9,066 CFU/mL of oyster homogenate with an average of 2,197 CFU/mL. In St. Charles Bay, the abundance of presumptive *V. vulnificus* ranged from not detectable to 4,300 CFU/mL of oyster homogenate with an average of 1,241 CFU/mL. Not detectable values were recorded for both sites during the April 8 sampling trip when water temperatures were cooler (see Figure 3). The 9,066 CFU/mL and 4,300 CFU/mL maximums were recorded during the April 29 and July 29 sampling trips, respectively. It was observed that oysters from Shellbank Reef were generally larger than oysters from St. Charles Bay, and the larger oysters proved easier to process and homogenize. Thus, the differences in presumptive *V. vulnificus* abundance could be the result of homogenization efficiency.

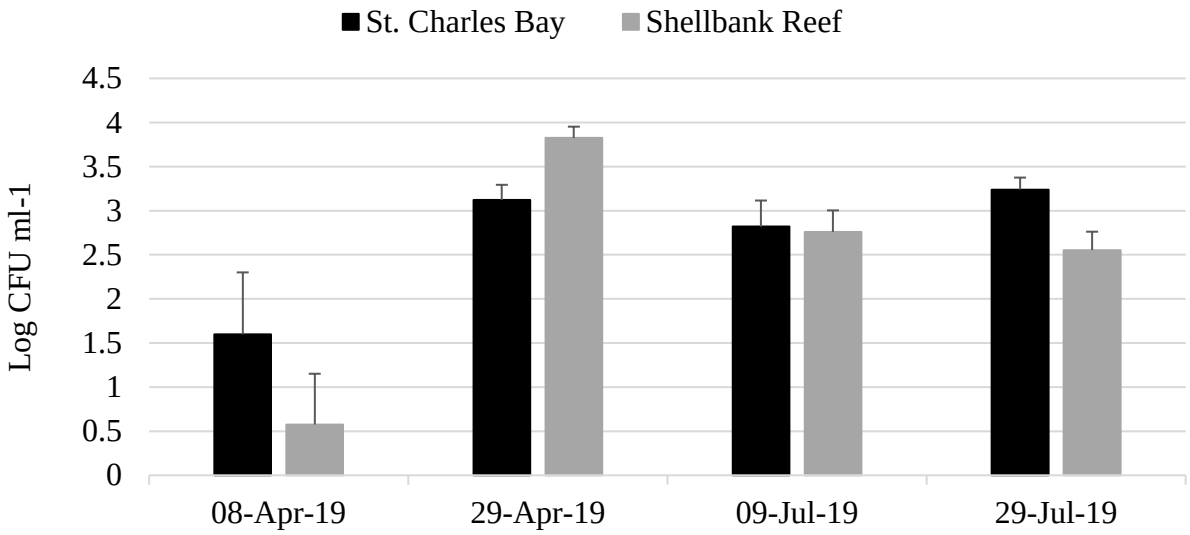

Figure 5. The variation in the log-transformed abundance of presumptive *V. vulnificus* (CFU/mL oyster homogenate) over the three month study period in Shellbank Reef and St. Charles Bay. Columns show the average abundance (N = 4 oysters per site) and error bars show the standard error.

Dermo abundance

The infection intensity of *P. marinus* varied minimally over the three month study (Figure 6). In St. Charles Bay and Shellbank Reef, the infection intensity of *P. marinus* ranged from 0 (not detectable) to 1.67 (light infection). Variations in intensity were not correlated with changes in environmental parameters or *V. vulnificus* abundance. The infection intensity was clearly lower in oysters from Shellbank Reef for all five sampling dates, although it was only significantly different for three dates (April 8, July 9, and July 29, 2019). Thus, the infection intensity was always lower in the restored reef (i.e., Shellbank Reef). This finding could suggest that sedimentation is related

to infection intensity as a previous report indicated that higher reefs are less impacted by sedimentation and experience less mortality (Colden *et al.* 2017).

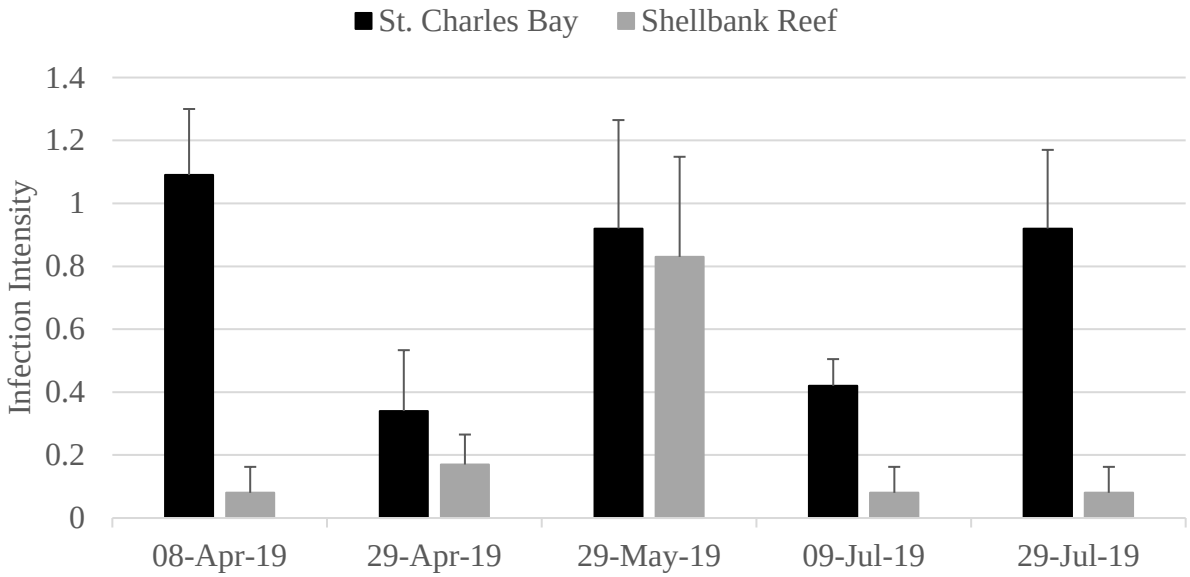

Figure 6. Variation in the infection intensity of *P. marinus* over the three month study period in Shellbank Reef and St. Charles Bay. Columns show the average infection intensity (N = 4 oysters per site) and error bars show the standard error.

V. vulnificus confirmation

A species-specific PCR test was used to confirm the identity of presumptive *V. vulnificus* isolates. In total, 120 presumptive *V. vulnificus* isolates were subcultured, cryopreserved, and tested for the presence of the *vvhA* species-specific gene target (see Appendix A for complete PCR results). Fewer than half of the isolates (54/120 or 45%) tested positive for the 519 bp *vvhA* gene target (Figure 7). Isolates confirmed as *V. vulnificus* were divided between St. Charles Bay (N=25) and Shellbank Reef (N=29). This finding indicated that the VVX media, when incubated at 30ºC, was semi-selective rather than selective (i.e., it permitted the growth of non-target species). Griffitt and Grimes reported that VVX was most selective at 37ºC (Griffitt & Grimes, 2013), but that temperature would have selected against the growth of most strains adapted to life in the marine environment and thus underestimate the abundance of *V. vulnificus*. Alternative and more accurate methods such as colony blot hybridization and real-time PCR are available (Kaysner & DePaola, 2004) but the cost and labor of these methods was prohibitive in this pilot study.

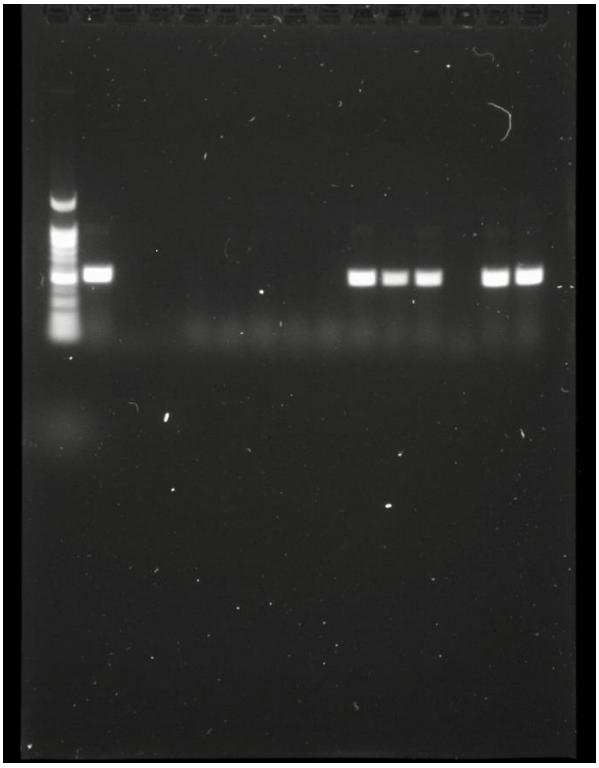

Figure 7. Example of a gel showing the results of the *vvhA* PCR test. Bright bands indicate isolates that tested positive for the marker while the absence of a bright bands indicate isolates that tested negative for the marker. The sequence of bright bands on the far left is a ladder used as a size reference; the brightest band on the ladder is 500 bp. The first bright band shows the positive control *V. vulnificus* ATCC 27562.

Isotope results

The plots of isotope values against distance across the shell indicated fluctuations that are at least partially responsive to environmental changes in ambient salinity and temperature (Figures 8 and 9). These plots function similarly to a time series, although the distance measurements are not uniformly aligned with true time nor identical across shells given variations in raster placement to avoid bore holes and individual variation in shell growth rates. In addition, the rasters that were milled in this study were larger than those milled for prior work (Walther and Rowley 2013) because the instrumentation for the current analyses required larger sample masses for reliable isotopic analyses. The temporal resolution of the subsamples is thus coarser and likely averaging out subseasonal to seasonal fluctuations that might be evident with higher resolution sampling.

Regardless of these limitations and inability to identify seasonal fluctuations that might otherwise be detected with higher resolution sampling, the trends indicated trends that were largely expected given the environmental time series recorded over the year prior to collection. Many shells showed dips on the order of 2‰ in both ratios, often followed by recovery at the final portion of the series in the most recent material grown prior to harvest. These patterns match what would be expected given the sharp decline in salinity from 20 to 5 at the Copano West station and 35 to 10 at the Copano East station in late summer 2018, which were then followed by slow increases in salinity over the subsequent year. Prior modelling relating oyster shell $\delta^{13}C$ values to salinity in the same geographical region estimated nan approximate 0.17‰ drop in $\delta^{13}C$ with every decrease of salinity by one. Thus, the decline in salinity by approximately 15 in Copano West would correspond to a downward shift in $\delta^{13}C$ values of 2.6‰, which is comparable to shifts observed in Shellbank Reef individuals (e.g. SHR22L which recorded a decline in $\delta^{13}C$ values from -3.4‰ to -5.8‰, or a downward shift of 2.4‰).

An additional line of evidence that the isotope records were primarily responsive to salinity is the positive relationships among the two values within each shell (Figure 10), indicating that peaks and valleys in both signatures were simultaneous. Negative relationships would indicate opposite fluctuations (e.g. $\delta^{13}C$ values increase while $\delta^{18}O$ values decrease) while no relationship would indicate the fluctuations in either signature were not related. However, all 6 shells examined showed positive relationships with slopes near or above 1. This type of positive relationship is expected if salinity is the primary driver of both signatures, given that influxes of fresh water to estuarine systems delivers water with isotopically lower $\delta^{18}O$ values and lower $\delta^{13}C$ values in dissolved inorganic carbon derived from terrestrial sources (Atekwana *et al.* 2003; Dutton *et al.* 2005; Fry 2002; LeGrande and Schmidt 2006).

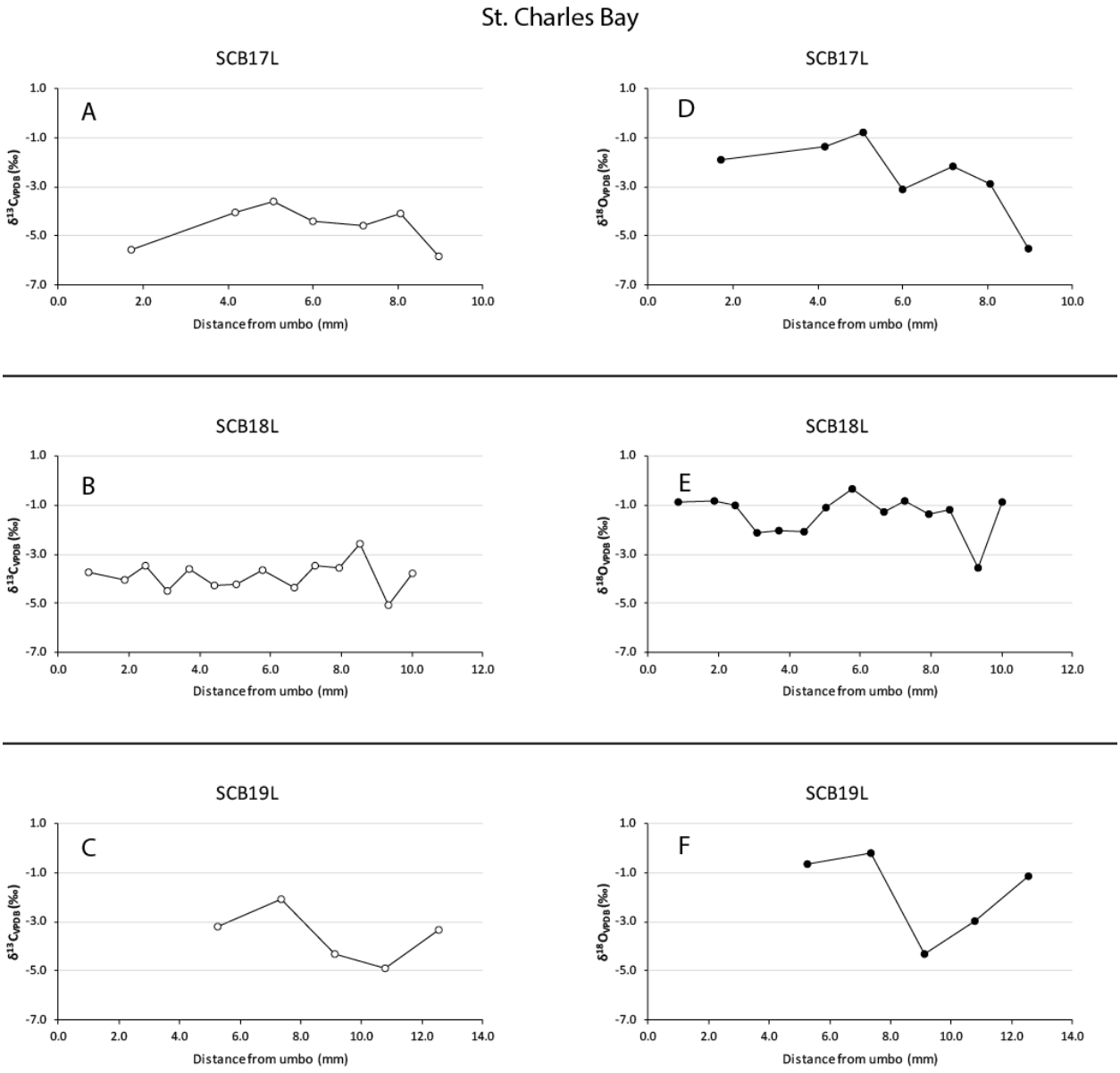

Figure 8. Time series of (A-C; open symbols) $\delta^{13}C$ and (D-F; closed symbols) $\delta^{18}O$ values across three shells from St. Charles Bay. Isotope values from the same shell are adjacent. Isotope values are plotted against the distance from the umbo or oldest portion of the shell, with distance serving as a proxy for time from oldest to newest material (left to right).

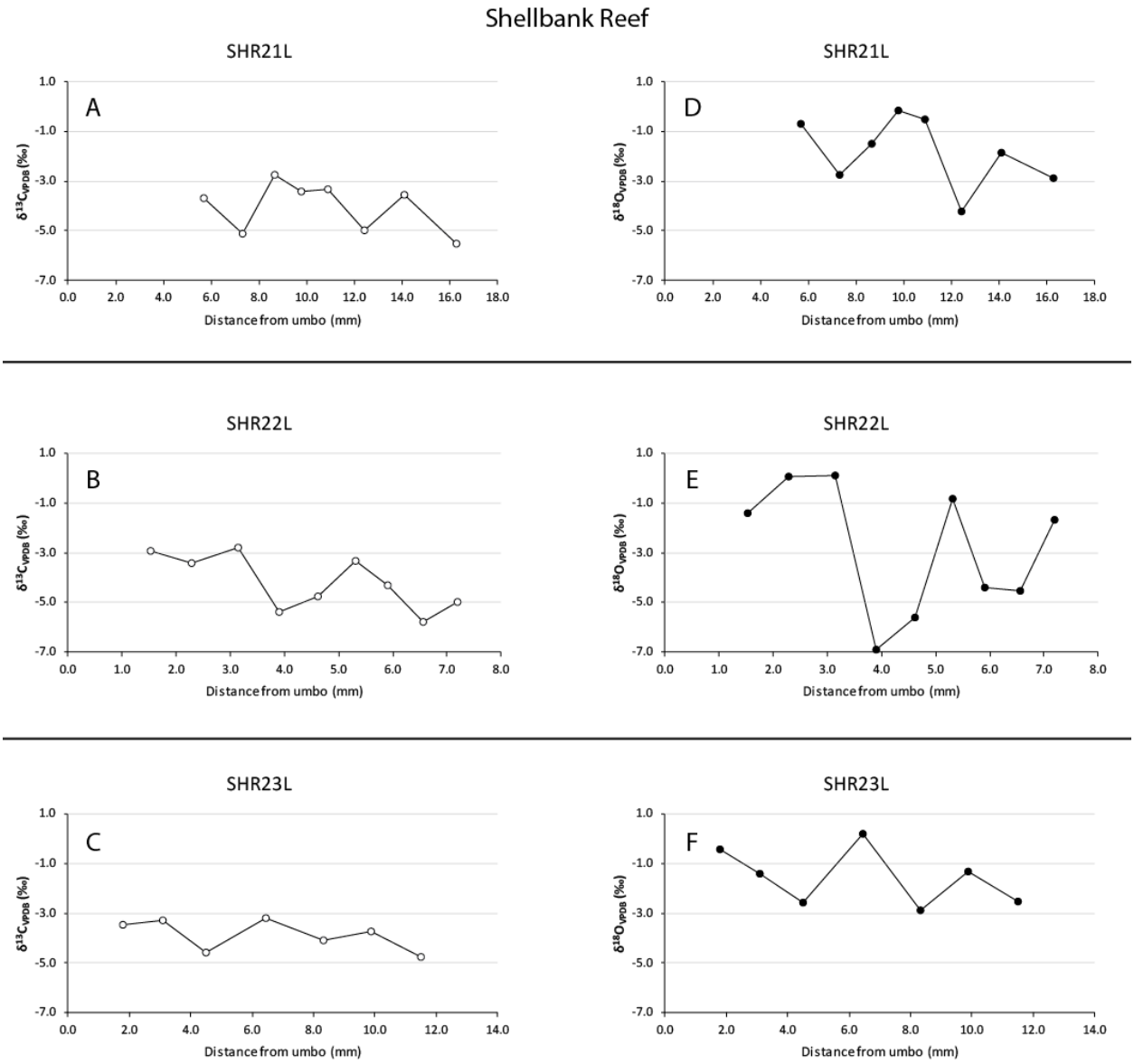

Figure 9. Time series of (A-C; open symbols) $\delta^{13}C$ and (D-F; closed symbols) $\delta^{18}O$ values across three shells from Shellbank Reef. Isotope values from the same shell are adjacent. Isotope values are plotted against the distance from the umbo or oldest portion of the shell, with distance serving as a proxy for time from oldest to newest material (left to right).

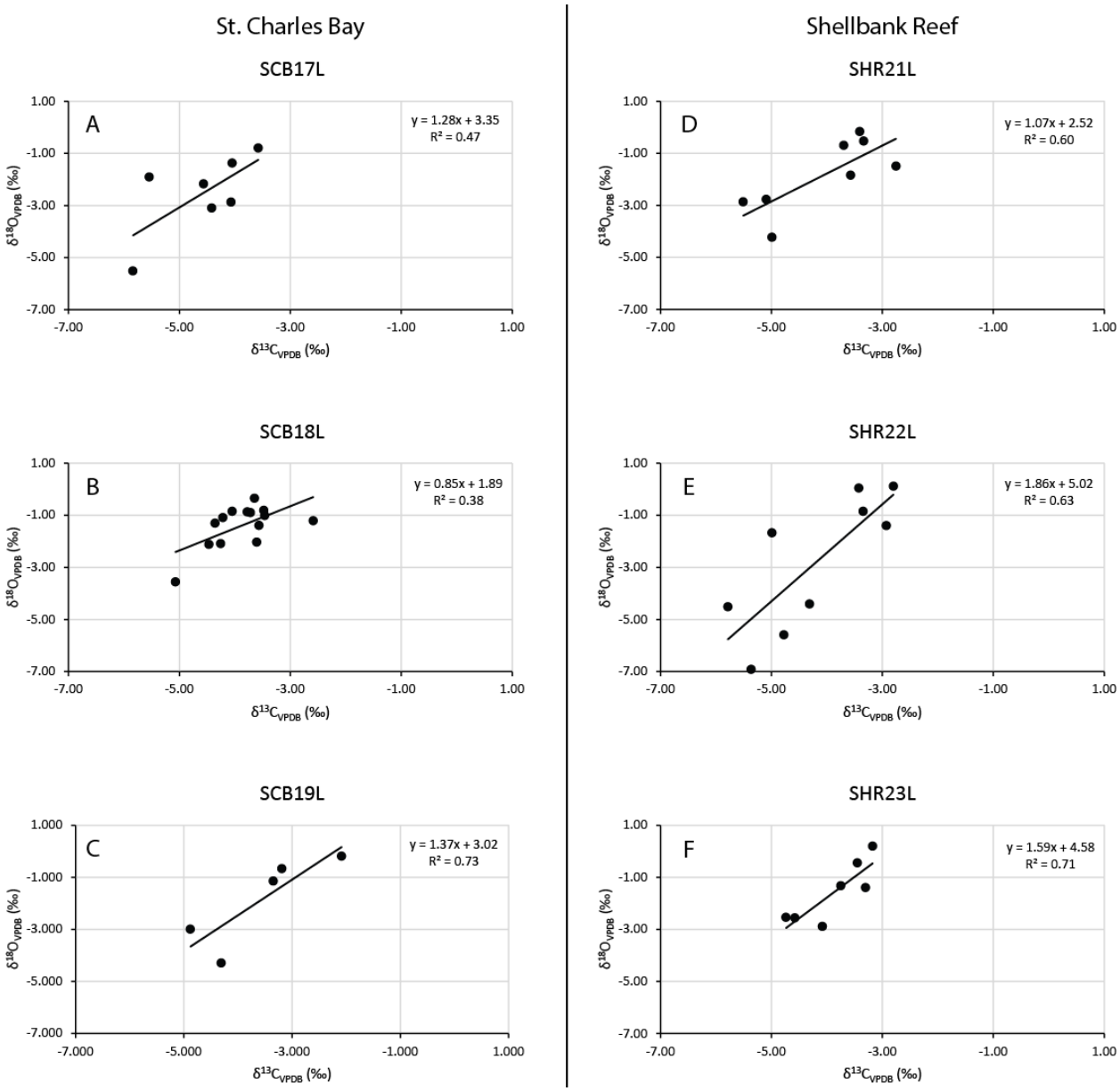

Figure 10. Regressions between $\delta^{13}C$ and $\delta^{18}O$ values for subsamples from individual shells from (A-C) St. Charles Bay and (D-F) Shellbank Reef. Linear regression equations and the associated R^2 values are indicated for each shell.

Because the overall trends in salinity were similar between the two monitoring stations, it is also not surprising that there were no obvious differences in isotope patterns between Shellbank Reef and St. Charles Bay. Although the absolute magnitude of the salinity maxima differed, the temporal variation was comparable at both sites, and isotope records in shells were therefore expected to exhibit similar magnitudes of variation across individuals from each site. One-way repeated measures analyses of variance did not identify statistically significant differences in values of either $\delta^{18}O$ ($F(13,5)=1.05$, $p=0.41$) or $\delta^{13}C$ ($F(13,5)=1.0$, $p=0.44$) among shells. The lack of statistically significant differences among all individuals also indicated that there were no systematic differences among sites in isotope records. Boxplots (Figure 11.) showed substantial overlap in distributions of $\delta^{18}O$ and $\delta^{13}C$ values across shells regardless of sampling location. Again, the relative similarities in environmental conditions in the prior year before sampling would be expected to result in comparable isotope variations in all shells from both locations, and these similarities were observed. Higher resolution sampling in future work would most likely reveal seasonal fluctuations in isotopes (particularly $\delta^{18}O$ values which are more sensitive to temperature than $\delta^{13}C$ values) in addition to punctuated salinity changes following events such as hurricanes.

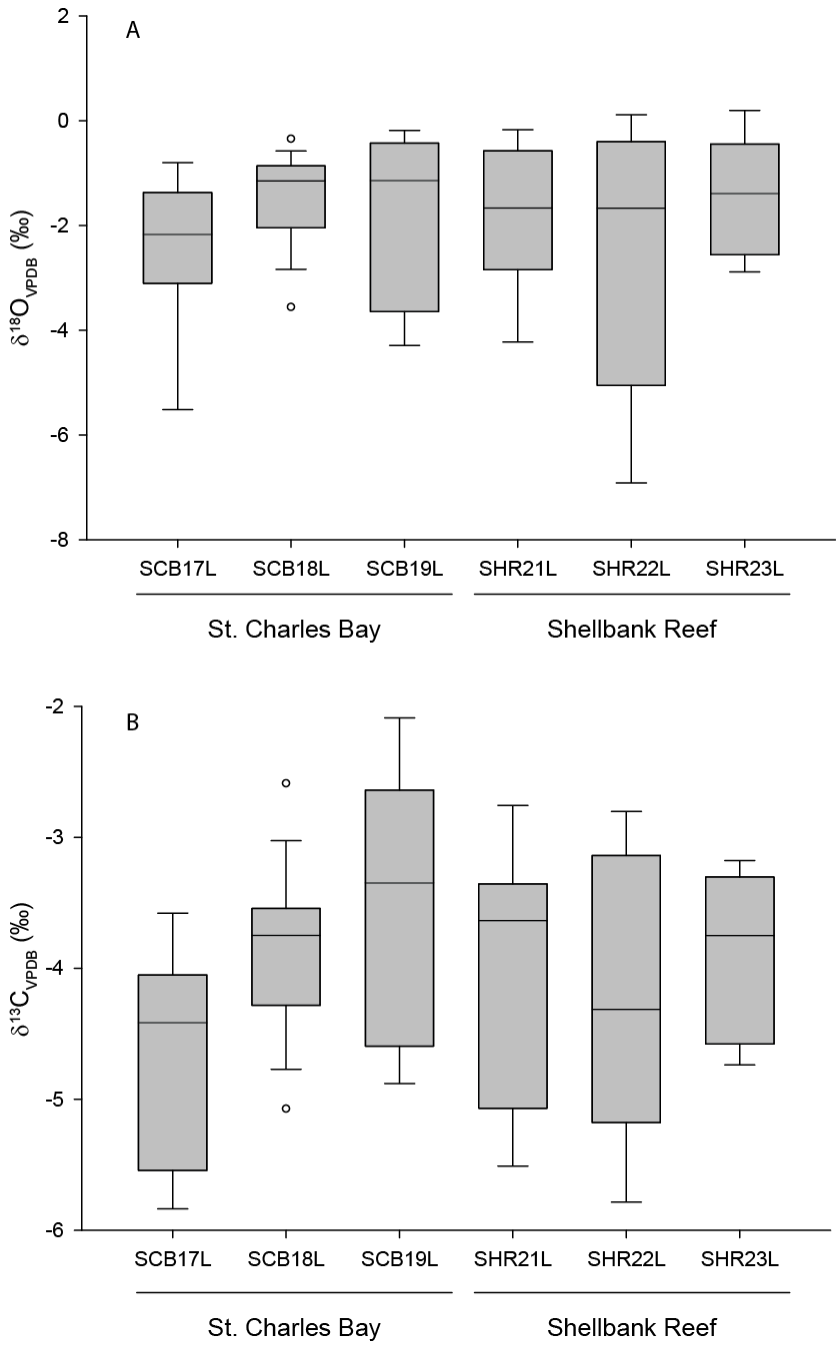

Figure 11. Boxplots depicting variations in (A) $\delta^{18}O$ and (B) $\delta^{13}C$ values within individual shells from St. Charles Bay and Shellbank Reef.

CONCLUSIONS

Oyster reefs are subject to periodic pulses of freshwater. This study attempted to assess how two distinct reefs, Shellbank Reef and St. Charles Bay, responded to freshwater intrusion. The analysis of historical salinity monitoring data and isotopic signatures indicated that both reefs experienced similar salinity fluctuations. Thus, this study afforded a comparison of a natural reef (St. Charles Bay) versus a restored reef (Shellbank Reef) that have experienced similar magnitudes of freshwater intrusion. The abundance of the bacterium *V. vulnificus* and the infection intensity of parasite *P. marinus* (i.e., Dermo) served as proxies for monitoring changes in oyster microbiota. The abundance of *V. vulnificus* was not significantly different between reefs but the Dermo infection intensity was significantly lower in the restored reef. This decreased infection intensity may relate to the reef height as higher restored reefs have been shown to experience less sedimentation and mortality.

REFERENCES

Atekwana, E.A., Tedesco, L.P., and Jackson, L.R. (2003). Dissolved inorganic carbon (DIC) and hydrologic mixing in a subtropical riverine estuary, southwest Florida, USA. *Estuaries* **26**, 1391-1400.

Colden, A.M., Latour, R.J., and Lipcius, R.N. (2017). Reef height drives threshold dynamics of restored oyster reefs. *Marine Ecology Progress Series* **582**, 1-13.

Dutton, A., Wilkinson, B.H., Welker, J.M., Bowen, G.J., and Lohmann, K.C. (2005). Spatial distribution and seasonal variation in $^{18}O/^{16}O$ of modern precipitation and river water across the conterminous USA. *Hydrological Processes* **19**, 4121-4146.

Englen, M.D., and Kelley, L.C. (2000). A rapid DNA isolation procedure for the identification of *Campylobacter jejuni* by the polymerase chain reaction. *Letters in Applied Microbiology* **31**, 421-426.

Froelich, B.A., Williams, T.C., Noble, R.T., and Oliver, J.D. (2012). Apparent loss of *Vibrio vulnificus* from North Carolina oysters coincides with a drought-induced increase in salinity. *Applied and Environmental Microbiology* **78**, 3885-3889.

Fry, B. (2002). Conservative mixing of stable isotopes across estuarine salinity gradients: a conceptual framework for monitoring watershed influences on downstream fisheries production. *Estuaries* **25**, 264-271.

Gillikin, D.P., Lorrain, A., Bouillon, S., Willenz, P., and Dehairs, F. (2006). Stable carbon isotopic composition of *Mytilus edulis* shells: relation to metabolism, salinity, $\delta^{13}C_{DIC}$ and phytoplankton. *Organic Geochemistry* **37**, 1371-1382.

Griffitt, K.J., and Grimes, D.J. (2013). A novel agar formulation for isolation and direct enumeration of *Vibrio vulnificus* from oyster tissue. *Journal of Microbiological Methods* **94**, 98-102.

Kaysner, C.A., and DePaola, A. (2004). Bacteriological Analytical Manual, Chapter 9: *Vibrio*. (Federal Drug Administration)

LeGrande, A.N., and Schmidt, G.A. (2006). Global gridded data set of the oxygen isotopic composition in seawater. *Geophysical Research Letters* **33**, L12604, doi:10.1029/2006GL026011.

Ostermann, D.R., and Curry, W.B. (2000). Calibration of stable isotopic data: an enriched $\delta^{18}O$ standard used for source gas mixing detection and correction. *Paleoceanography* **15**, 353-360.

Pollack, J.B., Cleveland, A., Palmer, T.A., Reisinger, A.S., and Montagna, P.A. (2012). A restoration suitability index model for the eastern oyster (*Crassostrea virginica*) in the Mission-Aransas estuary, TX, USA. *PLoS ONE* **7**, e40839.

Ray, S.M. (1952). A culture technique for the diagnosis of infections with *Dermocystidium marinum* Mackin, Owen, and Collier in oysters. *Science* **116**, 360-361.

Sharp, Z. (2007). 'Principles of stable isotope geochemistry.' (Pearson Prentice Hall: Upper Saddle River, NJ.)

Strom, M.S., and Paranjpye, R.N. (2000). Epidemiology and pathogenesis of *Vibrio vulnificus*. *Microbes and Infection* **2**, 177-188.

Surge, D., Lohmann, K.C., and Dettman, D.L. (2001). Controls on isotopic chemistry of the American oyster, *Crassostrea virginica*: implications for growth patterns. *Palaeogeography Palaeoclimatology Palaeoecology* **172**, 283-296.

Turner, J.W., Malayil, L., Guadagnoli, D., Cole, D., and Lipp, E.K. (2014). Detection of *Vibrio parahaemolyticus*, *Vibrio vulnificus* and *Vibrio cholerae* with respect to seasonal fluctuations in temperature and plankton abundance. *Environmental Microbiology* **16**, 1019-1028.

Walther, B.D., and Rowley, J.L. (2013). Drought and flood signals in subtropical estuaries recorded by stable isotope ratios in bivalve shells. *Estuarine, Coastal and Shelf Science* **133**, 235-243.

APPENDIX

Appendix A. Complete record of the *vvhA* PCR results, showing the provenance of the 120 presumptive *V. vulnificus* isolates: oyster and isolate number from either St. Charles Bay (SCB) or Shellbank Reef (SHR) with detection of the 519 bp gene marker noted as present (1) or absent (0).

Location	Isolate	*vvhA*
SCB	Oyster 10: Isolate 1	1
SCB	Oyster 10: Isolate 2	1
SCB	Oyster 10: Isolate 3	0
SCB	Oyster 10: Isolate 4	0
SCB	Oyster 10: Isolate 5	1
SCB	Oyster 11: Isolate 1	1
SCB	Oyster 11: Isolate 2	1
SCB	Oyster 11: Isolate 3	1
SCB	Oyster 11: Isolate 4	0
SCB	Oyster 11: Isolate 5	1
SCB	Oyster 12 : Isolate 1	0
SCB	Oyster 12 : Isolate 2	0
SCB	Oyster 12 : Isolate 3	1
SCB	Oyster 12 : Isolate 4	0
SCB	Oyster 12 : Isolate 5	1
SHR	Oyster 13 : Isolate 1	0
SHR	Oyster 13 : Isolate 2	1
SHR	Oyster 13 : Isolate 3	1
SHR	Oyster 13 : Isolate 4	1
SHR	Oyster 13 : Isolate 5	1
SHR	Oyster 14 : Isolate 1	1
SHR	Oyster 14 : Isolate 2	1
SHR	Oyster 14 : Isolate 3	0
SHR	Oyster 14 : Isolate 4	1
SHR	Oyster 14 : Isolate 5	1
SHR	Oyster 15 : Isolate 1	1
SHR	Oyster 15 : Isolate 2	1
SHR	Oyster 15 : Isolate 3	0
SHR	Oyster 15 : Isolate 4	1
SHR	Oyster 15 : Isolate 5	0
SHR	Oyster 16 : Isolate 1	1
SHR	Oyster 16 : Isolate 2	1

SHR	Oyster 16 : Isolate 3	1
SHR	Oyster 16 : Isolate 4	1
SHR	Oyster 16 : Isolate 5	1
SCB	Oyster 2: Isolate 1	0
SCB	Oyster 2: Isolate 2	0
SCB	Oyster 2: Isolate 3	0
SCB	Oyster 2: Isolate 4	0
SCB	Oyster 2: Isolate 5	1
SCB	Oyster 25: Isolate 1	0
SCB	Oyster 25: Isolate 2	0
SCB	Oyster 26: Isolate 1	0
SCB	Oyster 26: Isolate 2	0
SCB	Oyster 26: Isolate 3	0
SCB	Oyster 26: Isolate 4	1
SCB	Oyster 26: Isolate 5	1
SCB	Oyster 27: Isolate 1	1
SCB	Oyster 27: Isolate 2	0
SCB	Oyster 27: Isolate 3	1
SCB	Oyster 27: Isolate 4	0
SCB	Oyster 27: Isolate 5	1
SCB	Oyster 28: Isolate 1	1
SCB	Oyster 28: Isolate 2	1
SCB	Oyster 28: Isolate 3	1
SCB	Oyster 28: Isolate 4	0
SCB	Oyster 28: Isolate 5	1
SHR	Oyster 29: Isolate 1	1
SHR	Oyster 29: Isolate 2	1
SHR	Oyster 29: Isolate 3	1
SHR	Oyster 29: Isolate 4	0
SHR	Oyster 29: Isolate 5	0
SHR	Oyster 30: Isolate 1	0
SHR	Oyster 30: Isolate 2	0
SHR	Oyster 30: Isolate 3	0
SHR	Oyster 30: Isolate 4	0
SHR	Oyster 30: Isolate 5	0
SHR	Oyster 31: Isolate 1	1
SHR	Oyster 31: Isolate 2	1
SHR	Oyster 31: Isolate 3	1
SHR	Oyster 31: Isolate 4	1
SHR	Oyster 31: Isolate 5	1

SHR	Oyster 32: Isolate 1	1
SHR	Oyster 32: Isolate 2	1
SCB	Oyster 33: Isolate 1	0
SCB	Oyster 33: Isolate 2	0
SCB	Oyster 33: Isolate 3	0
SCB	Oyster 33: Isolate 4	0
SCB	Oyster 33: Isolate 5	0
SCB	Oyster 34: Isolate 1	0
SCB	Oyster 34: Isolate 2	0
SCB	Oyster 34: Isolate 3	0
SCB	Oyster 34: Isolate 4	0
SCB	Oyster 34: Isolate 5	0
SCB	Oyster 35: Isolate 1	0
SCB	Oyster 35: Isolate 2	0
SCB	Oyster 35: Isolate 3	0
SCB	Oyster 35: Isolate 4	0
SCB	Oyster 35: Isolate 5	0
SCB	Oyster 36: Isolate 1	0
SCB	Oyster 36: Isolate 2	0
SCB	Oyster 36: Isolate 3	1
SCB	Oyster 36: Isolate 4	1
SCB	Oyster 36: Isolate 5	1
SHR	Oyster 37: Isolate 1	0
SHR	Oyster 37: Isolate 2	1
SHR	Oyster 37: Isolate 3	1
SHR	Oyster 38: Isolate 1	0
SHR	Oyster 39: Isolate 1	0
SHR	Oyster 39: Isolate 2	0
SHR	Oyster 39: Isolate 3	0
SHR	Oyster 39: Isolate 4	0
SHR	Oyster 39: Isolate 5	0
SCB	Oyster 4: Isolate 1	0
SCB	Oyster 4: Isolate 2	0
SHR	Oyster 40: Isolate 1	0
SHR	Oyster 40: Isolate 2	0
SHR	Oyster 40: Isolate 3	0
SHR	Oyster 40: Isolate 4	1
SHR	Oyster 40: Isolate 5	0
SHR	Oyster 8: Isolate 1	0
SHR	Oyster 8: Isolate 2	0

SHR	Oyster 8: Isolate 3	0
SHR	Oyster 8: Isolate 4	0
SHR	Oyster 8: Isolate 5	0
SCB	Oyster 9: Isolate 1	1
SCB	Oyster 9: Isolate 2	1
SCB	Oyster 9: Isolate 3	0
SCB	Oyster 9: Isolate 4	0
SCB	Oyster 9: Isolate 5	1